Proceedings of the International Conference on

stepping motors and systems

Leeds 19th–20th September 1979

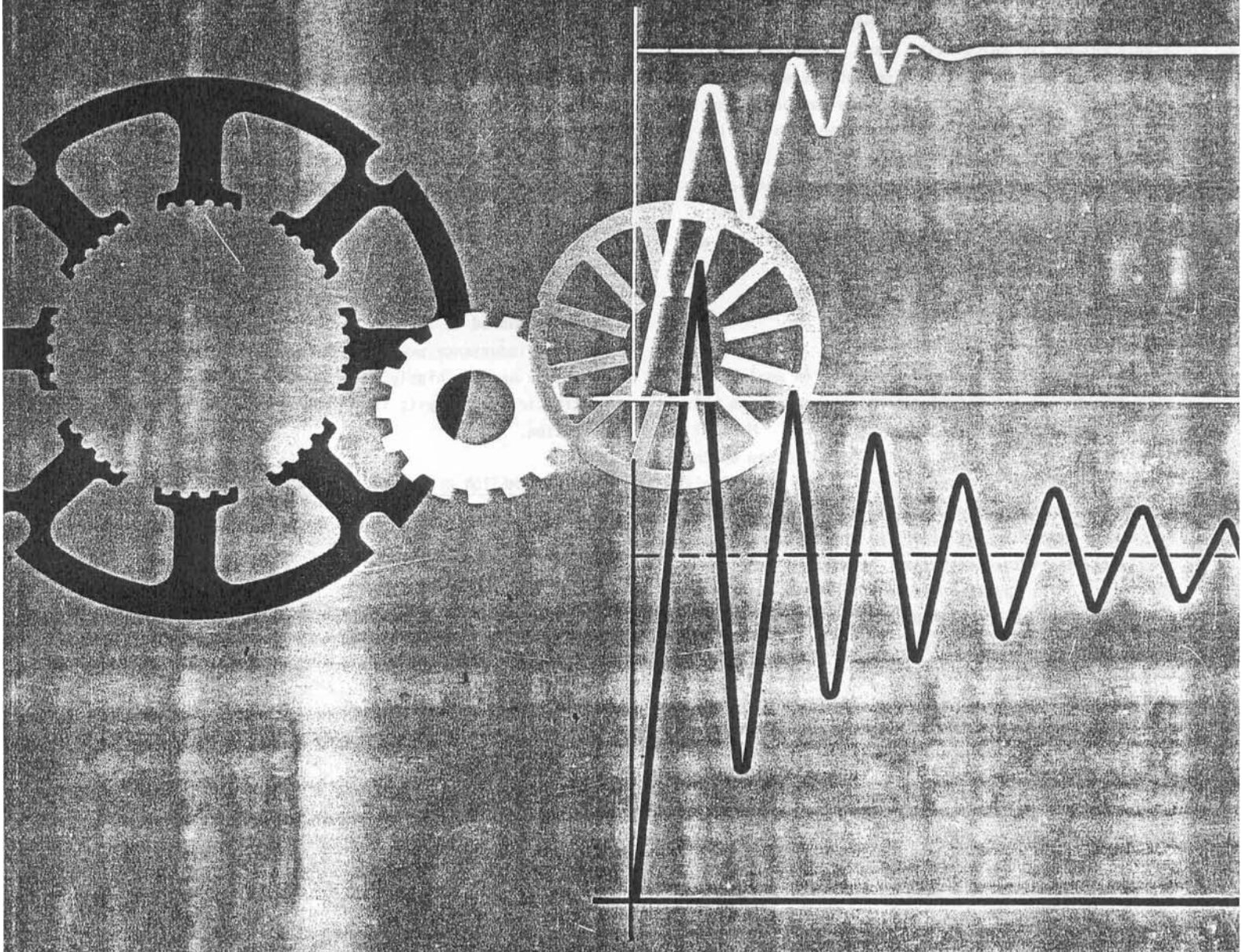

The Department of Electrical and Electronic Engineering, University of Leeds

ANALYTICAL ESTIMATION OF THE MINIMUM AND MAXIMUM INDUCTANCES OF A DOUBLE-SALIENT MOTOR

J Čorda and J M Stephenson

Department of Electrical and Electronic Engineering
University of Leeds

1. INTRODUCTION

The minimum and maximum inductances corresponding to the two extreme rotor positions, when the axis of excited pole is aligned with the rotor interpolar axis and when it is aligned with the rotor pole axis, are very important parameters in determining the behaviour of doubly-salient motors. This paper presents a simple method for calculating these parameters in terms of the geometric proportions of the machine including the effects of the distribution of the exciting coils. The magnetic configuration of a doubly-salient motor of typical dimensional proportions is considered and the results obtained by this method are compared with those found by numerical field solution and experimentally. An allowance for fringe flux at the ends of the core is made.

2. GENERAL APPROACH

A great deal of work has been done on analytically determining the magnetic permeance and force between toothed structures of stepping motors. Much of this springs from the work of F W Carter[1] based on the Schwarz-Christoffel transformation. Some of Carter's unpublished work has been modified and used as a basis for a very comprehensive numerical analysis of identically double-slotted structures by Mukherji and Neville[2]. This approach has been recently adapted for convenient application to stepping motors by Ward and Lawrenson[3]. Jones'[4] Schwarz-Christoffel transformation, to evaluate permeance and forces, was applicable to identical double-toothed structures where the gap is small compared to the tooth dimensions. Chai[5] has developed permeance formulae based on the assumption of the simple pattern of the field between toothed structures which consists of straight lines segments and concentric circular arcs. It is important to note that Jones' and Chai's results for the permeance are in very good agreement when the air-gap length is small compared to the other dimensions.

However, all the methods above are based on the analysis of rectangular teeth and slots on the stator and rotor and neglect the distribution of the exciting coils on the teeth or assume them to be remote from the teeth. These assumptions may not be justifiable in a doubly-salient motor having excitation coils on the stator poles (teeth) and where profiles of the stator and rotor poles and interpolar spaces are not rectangular.

The agreement of Jones' and Chai's results suggests that the assumption that field lines consist of straight line segments and circular arcs might be used even in the presence of distributed coils where the air-gap length is small compared with the other dimensions. Thus in the method for estimating the minimum inductance described below it is assumed that the field lines conform to this assumption and that the magnetic permeability of the iron is infinite with the flux lines entering the iron surface perpendicularly. The assumption of infinite permeability of the iron is realistic in this position, because the air paths of the field lines are very long and the mmf drop in the iron is small compared to that in the air. However, in the maximum inductance position the air-gap is small and the iron becomes highly saturated. A classical magnetic circuit analysis is therefore used in this position.

3. ESTIMATION OF THE MINIMUM INDUCTANCE

Fig 1 shows a sketch of the field pattern of the

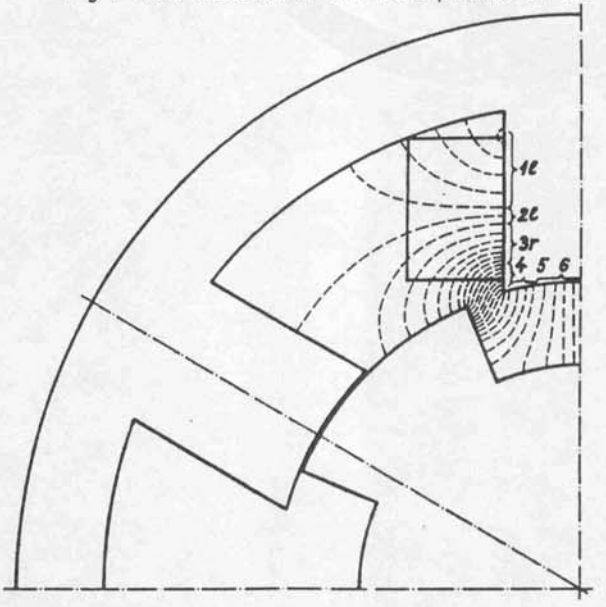

Fig. 1 Sketch of the field pattern in minimum inductance position

magnetic configuration corresponding to the minimum inductance position for a motor of typical dimensional proportions. It is assumed that the field inside the machine is plane-parallel with respect to the plane of the figure and can therefore be considered in two dimensions. The field effects at the ends of the machine (in the third dimension) are considered separately. Since it is assumed that the magnetic permeability of iron is infinite, the magnetic potential of the iron except for the poles of the excited phase are zero. The field lines may be devided into two groups: those which pass to the rotor and those which do not. This latter group consists of the lines which lead from the excited stator pole side to the stator back of core (path 1ℓ) and lines which lead from the stator pole side to the adjacent pole (path 2ℓ). The first group consists of the lines which lead from the stator pole side to the rotor pole surface (path 3r), lines which lead from the stator pole side to the rotor pole side (path 4), lines which lead from the stator pole face to the rotor pole side (path 5) and lines which lead from the stator pole face to the rotor interpolar surface (path 6).

It should be noted that each of the field lines in the paths 1ℓ, 2ℓ and 3r is linked with a different number of turns. (Such partial linkages have not been treated in the previously published methods for determination of inductances of doubly-salient machines.) The lines of path 4, 5 and 6 are approximately linked with all the turns and are assumed to link perfectly.

In order to allow an analytical solution it is assumed that the conductors are uniformly distributed over the coil cross-section and the field lines are approximated as follows: It is clear from the path length and linked amp-turns that the flux-linkage of the path 2ℓ is very small in comparison with the flux-linkage of the paths 4, 5 and 6. This also applies to the flux-linkages of the path 1 and the outer region of the path 3r, which are small compared with the flux-linkages of the paths 4, 5, 6 and the inner region of the path 3r, either because of the amount of amp-turns or because of the length of the field lines. Therefore, in calculating the total inductance, a large error will not be incurred even if a gross approximation is made to the mapping of the lines of path 2ℓ. Thus the path 2ℓ may be associated with paths 1 and 3r forming together paths 1 and 3 (Fig 2). The analytical determination of the position of the point O_ℓ is based on the condition that the ratio of the lengths of the lines from the point O_ℓ is equal to the ratio of amp-turns linked by them.

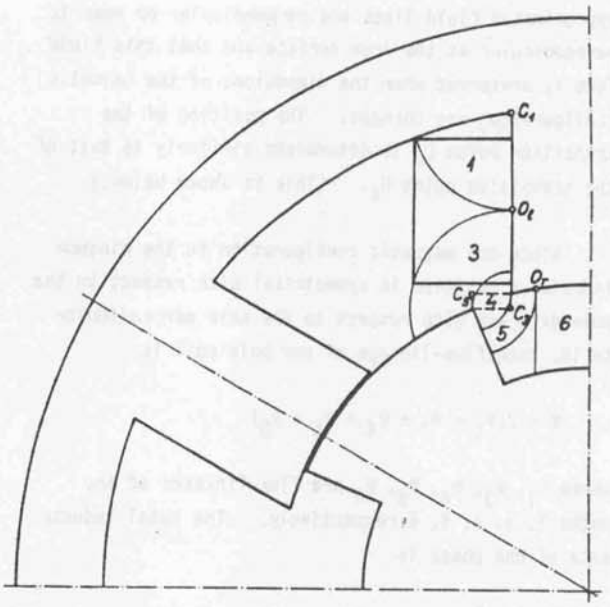

Fig. 2 Approximated flux paths

The results which are obtained by such rather extensive calculations show that point O_ℓ lies very near to the mid-point of the pole side. On the basis of this argument and the explanations given above about the values of the flux-linkages in the outer regions of the paths 1 and 3, the simple assumption that the point O_ℓ is at the mid-point of the coil side is justified. Obviously, these approximations are valid for calculating the total inductance whereas for calculating separately the leakage inductance and the inductance between the stator and the rotor, it would not be justified. Fig 2 shows the simplified field map inside the machine in which it is assumed that:

i) field lines of the path 1 consist of concentric circular arcs with the centre at the point C_1,

ii) field lines of the path 3 consist of the concentric circular arcs with the centre at the point C_3

iii) the field lines of path 4 are as given below,

iv) field lines of path 5 consist of concentric circular arcs with the centre at the point C_5, and

v) field lines of path 6 consist of parallel straight line segments.

Points C_1, C_3, C_5 are chosen on the basis that

approximated field lines are perpendicular or near to perpendicular at the iron surface and that this field form is preserved when the dimensions of the magnetic configuration are changed. The position of the transition point O_r is determined similarly to that of the transition point O_ℓ. (This is shown below.)

Since the magnetic configuration in the minimum inductance position is symmetrical with respect to the pole axis and with respect to the axis perpendicular to it, then flux-linkage of one pole coil is

$$\psi = 2(\psi_1 + \psi_3 + \psi_4 + \psi_5 + \psi_6)$$

where ψ_1, ψ_3, ψ_4, ψ_5, ψ_6 are flux-linkages of the paths 1, 3, 4, 5, 6 respectively. The total inductance of one phase is

$$L_o = 2\frac{\psi}{i}$$

because there are two poles per phase each of which has a coil with N/2 turns, where N is number of turns per phase.

$$L_o = \frac{4}{i}(\psi_1 + \psi_3 + \psi_4 + \psi_5 + \psi_6)$$

$$= 4(L_1 + L_3 + L_4 + L_5 + L_6)$$

$$= N^2 \mu_o \ell_F (P_1 + P_3 + P_4 + P_5 + P_6) \qquad (1)$$

$$= N^2 \mu_o \ell P_o \qquad (2)$$

where,

$$P_j = L_j / [\mu_o \ell_F (\tfrac{N}{2})^2], \quad (j = 1, 3, 4, 5, 6)$$

ℓ_F is the effective core length (see below),

$P_o = \frac{\ell_F}{\ell} \sum_j P_j$ is the total normalised equivalent minimum permeance.

3.1 Parameters of the Magnetic Configuration

The magnetic configuration is described by the following set of parameters

number of stator poles N_s,
number of rotor poles N_r,
stator pole arc s,
rotor pole arc r,
air-gap length g,
air-gap length of rotor interpolar space g_i,
rotor diameter d,
stator outside diameter d_o
back iron width c,
core length ℓ,
number of turns per phase N.

Let upper case letters represent normalised dimensional parameters, ie

$$G = \frac{g}{d_o},\ G_i = \frac{g_i}{d_o},\ D = \frac{d}{d_o},\ C = \frac{c}{d_o},\ L = \frac{\ell}{d_o}$$

The other angles and dimensions represented in Fig 3 can be represented in terms of the above parameters as follows

$$\phi = \frac{2\pi}{N_r}$$

$$\delta = \frac{2\pi}{N_s}$$

$$\gamma = \text{ang } H_2 C_1 E \simeq \frac{\pi}{2} - \frac{\delta}{2}$$

$$P = \frac{p}{d_o} = (\frac{D}{2} + G) \sin\frac{s}{2}$$

$$W = \frac{w}{d_o} = (\frac{D}{2} + G) \tan\frac{\delta}{2} - P$$

$$V = \frac{v}{d_o} = (\tfrac{1}{2} - C - \frac{\frac{D}{2} + G}{\cos\frac{\delta}{2}}) \frac{1}{\cos\frac{\delta}{2}}$$

$$Y = \frac{y}{d_o} = \frac{D}{2} + G - \frac{D}{2}\cos\frac{\phi - r}{2}$$

$$H = \frac{h}{d_o} = \frac{D}{2}\sin\frac{\phi - r}{2} - P$$

$$B = \frac{b}{d_o} = (\frac{D}{2} + G)\cos\frac{s}{2} - \frac{D}{2}\cos\frac{\phi - r}{2}$$

$$Q = \frac{q}{d_o} = \frac{V}{2}$$

$$U = \frac{u}{d_o} = \frac{W}{\tan\gamma}$$

$$M = \frac{m}{d_o} = U + Q$$

$$N = \frac{n}{d_o} = Y + Q$$

3.2 Calculation of Minimum Inductance Components

a) Component L_1

Fig 4 shows detail of the magnetic configuration for flux-path 1 where the broken line represents the approximated back of core surface. The flux-linkage of path 1 is small in comparison with the flux-linkages of paths 3, 4, 5 and 6, because the linked amp-turns become smaller as the field lines are nearer to the corner between the back of core and the pole. This is taken to justify the approximation that in calculating this particular inductance the small empty space between the pole winding and the

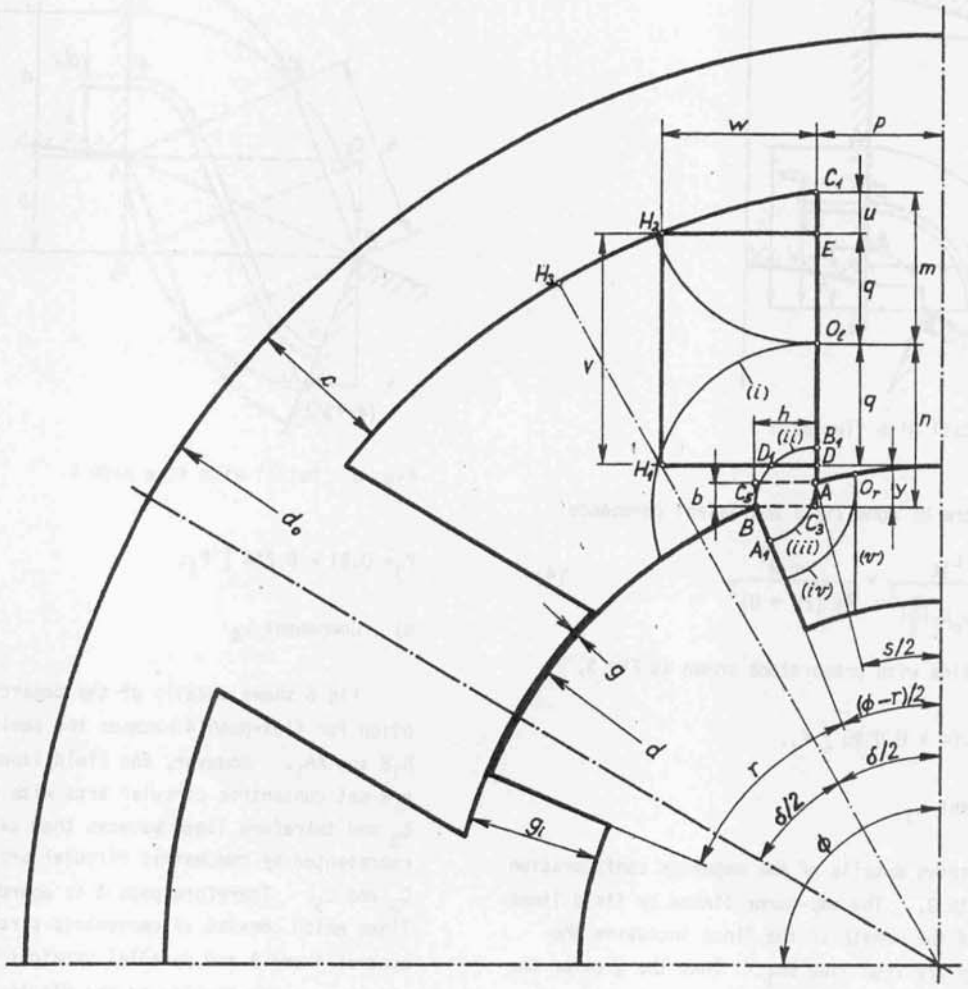

Fig. 3 Dimensional description of magnetic configuration

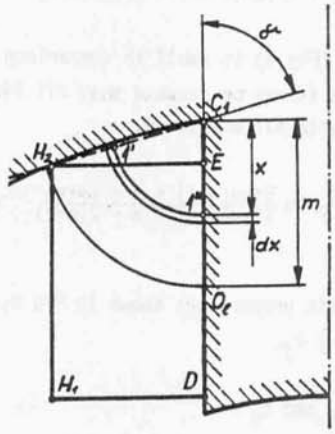

Fig. 4 Detail with flux path 1

back of core may be considered filled with pole winding turns.

The elementary flux-path 1'1" is linked with

$$\frac{\text{area } C_1 1'1'' C_1}{\text{area } C_1 H_2 H_1 D} \left(\frac{Ni}{2}\right) \simeq \frac{\frac{1}{2}\gamma x \, x}{w v + \frac{1}{2} w u} \left(\frac{Ni}{2}\right) \text{ amp-turns}$$

The field on the elementary flux-path 1'1" is

$$H_x = \frac{1}{\gamma x} \left(\frac{\frac{1}{2}\gamma x \, x}{w v + \frac{1}{2} w u} \left(\frac{Ni}{2}\right)\right)$$

The elementary flux-linkage is

$$d\psi_x = \left(\frac{\frac{1}{2}\gamma x \, x}{w v + \frac{1}{2} w u} \left(\frac{N}{2}\right)\right) \mu_o H_x \ell_F dx$$

Hence, L_1 is

$$L_1 = \frac{\int_{(o)}^{(m)} d\psi_x}{i} = \mu_o \ell_F \left(\frac{N}{2}\right)^2 \frac{\gamma \, m^4}{4 w^2 (2v + u)^2}$$

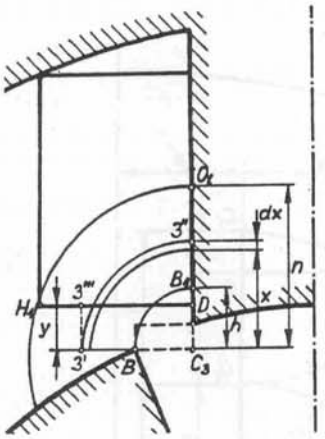

Fig. 5 Detail with flux path 3

or in the form of normalised equivalent permeance

$$P_1 = \frac{L_{1\ell}}{\mu_0 \ell_F (\frac{N}{2})^2} = \frac{\gamma M^4}{4W^2(2V + U)^2} \qquad (4)$$

For the machine with proportions shown in Fig 3,

$$P_1 = 0.04 = 0.0185 \sum P_j .$$

b) Component L_3

Fig 5 shows details of the magnetic configuration for flux-path 3. The amp-turns linked by field lines decrease and the length of the lines increases the further they are from line BB_1. Thus the greater the radius of the line, the smaller the contribution of flux-line to the value of inductance component L_3. This reasoning supports the approximation that the rotor pole surface may be represented by a straight line at right angle to the stator pole side through the point C_3. The elementary flux-path is linked with

$$\frac{wv\text{-area } D3''3'''D}{wv} (\frac{Ni}{2})$$

$$\approx \frac{wv+\text{area } D3'''3'C_3D-\text{area } C_3 3''3'C_3}{wv} (\frac{Ni}{2})$$

$$= \frac{wv + xy - \frac{x^2\pi}{4}}{wv} (\frac{Ni}{2}) \text{ amp-turns}$$

Using the procedure shown in Section 3.2(a)

$$P_3 = \frac{L_3}{\mu_0 \ell_F (\frac{N}{2})^2} = \frac{2}{\pi} \left\{ \ln \frac{N}{H} + \frac{2(N-H)Y}{WV} - \frac{(N^2 - H^2)}{4(WV)^2} (\pi WV - 2Y^2) - \frac{(N^3 - H^3)Y\pi}{6(WV)^2} + \frac{(N^4 - H^4)\pi^2}{64(WV)^2} \right\} \qquad (5)$$

For the machine with proportions shown in Fig 3,

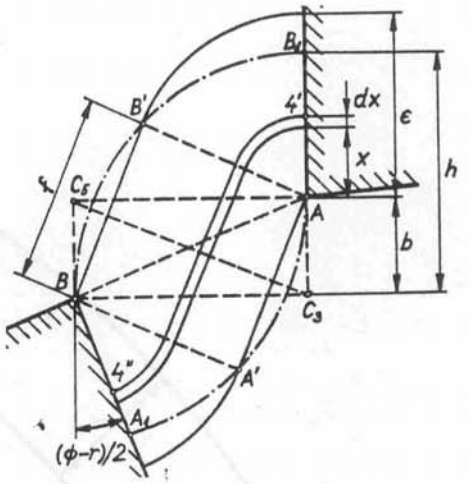

Fig. 6 Detail with flux path 4

$$P_3 = 0.51 = 0.246 \sum P_j .$$

c) Component L_4

Fig 6 shows details of the magnetic configuration for flux-path 4 between the semi-broken lines B_1B and AA_1. However, the field lines B_1B and AA_1 are not concentric circular arcs with centres C_3 and C_5 and therefore lines between them cannot be simply represented by concentric circular arcs with centres C_3 and C_5. Therefore path 4 is approximated by the lines which consist of concentric circular arcs with centres A and B and parallel straight line segments which are perpendicular to the diagonal C_3C_5 and of length

$$f = 2b \cos(C_3 AA') \approx 2b \frac{\phi - r}{2}$$

The radius

$$e = AB' = A'B = f/\tan(B'AB) \approx f/\tan(\phi - r)$$

Since area DB_1D_1D (Fig 3) is small in comparison with area DEH_2H_1D, then it may be assumed that all field lines are linked with all amp-turns.

$$P_4 = \frac{L_4}{\mu_0 \ell_F (\frac{N}{2})^2} = \frac{2}{\phi - r} \ln \frac{2\tan(\phi - r) + \pi - (\phi - r)}{2\tan(\phi - r) + \pi - 2(\phi - r)} \qquad (6)$$

For the machine with proportions shown in Fig 3,

$$P_4 = 0.51 = 0.236 \sum P_j .$$

d) Components L_5 and L_6

Fig 7 shows the magnetic configuration of flux-paths 5 and 6. If the field lines of path 5 consist

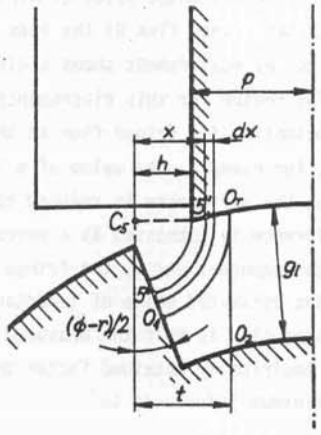

Fig. 7 Detail with flux paths 5 and 6

of concentric circular arcs with centre C_5, and the field lines of path 6 consist of parallel straight line segments, then the transition point O_r on the stator pole surface, is determined from the condition mentioned above, ie the length of the circular arc (field line) O_rO_1 is equal to length of straight line segment O_2O_r. The angle which corresponds to the circular arc may be approximately taken to be $\pi/2 - (\phi-r)/2$. Therefore, the condition that $O_rO_1 = O_2O_r$ is

$$t\left(\frac{\pi}{2} - \frac{\phi-r}{2}\right) = g_i \quad \therefore\ t = \frac{2\,g_i}{\pi - (\phi-r)}$$

The field lines of paths 5 and 6 are linked with all amp-turns. Hence

$$P_5 = \frac{L_5}{\mu_o \ell_F \left(\frac{N}{2}\right)^2} = \frac{2}{\pi - (\phi-r)} \ln \frac{2\,G_i}{H[\pi - (\phi-r)]} \qquad (7)$$

$$P_6 = \frac{L_6}{\mu_o \ell_F \left(\frac{N}{2}\right)^2} = \frac{P + H}{G_i} - \frac{2}{\pi - (\phi-r)} \qquad (8)$$

For the machine with proportions shown in Fig 3,

$P_5 = 0.55 = 0.255 \sum P_j$ and

$P_6 = 0.55 = 0.255 \sum P_j$.

3.3 Fringe Flux at the Ends of Core Effective Core Length

The inductance component due to field at the ends of core of the machine has not been considered in any previous publication on doubly-salient motors. The mathematical treatment of the fringe flux at the ends of core is extremely complicated, particularly for doubly-salient machines, and would require a 3-dimensional numerical field solution for a rigorous

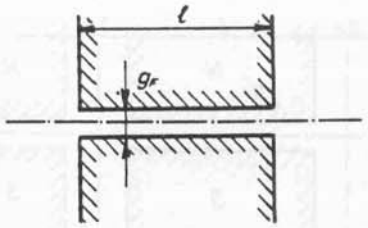

Fig. 8 Axial model of magnetic configuration with fictitious air-gap

treatment. This problem is the subject of continuing investigation but a simple method for making a very rough estimation of the contribution to the minimum inductance by the fringing flux is given below.

In Fig 8 the stator and rotor are represented by a pair of opposing faces with flanks extending to infinity and with a fictitious uniform air-gap, g_F, the length of which is chosen to be equal to the mean length of the lines (i), (ii), (iii), (iv) and (v) (Fig 3) (where the fringing is the most pronounced).

$$g_F = \frac{1}{5}\left[\frac{\pi}{2}n + \frac{\pi}{2}h + \left(\frac{\pi}{2} - \frac{\phi-r}{2}\right)h + g_i + g_j\right] \qquad (9)$$

It is assumed that the flux in the gap is uniform (ie fits the 2-dimensional field solution) to the end of the core and that the fringe flux at the ends of core is linked with all the turns.

The model in Fig 8 is symmetrical about the axis ss and therefore, the permeance of that model is equal to one half of the permeance of the model shown in Fig 9.

In the model in Fig 9 the fringing field is unlimited, ie the problem involves an infinite fringe. Carter[1] uses the Schwarz-Christoffel transformation to obtain an expression for fringeflux (effective core length) emphasizing that it is a matter of judgement how much of the computed fringe flux should be taken as effective. However, Carter's expressions for this case are very complex and are not suitable for

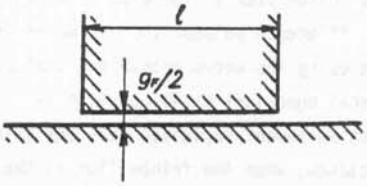

Fig. 9 'Half'-equivament of model with fictitious air-gap

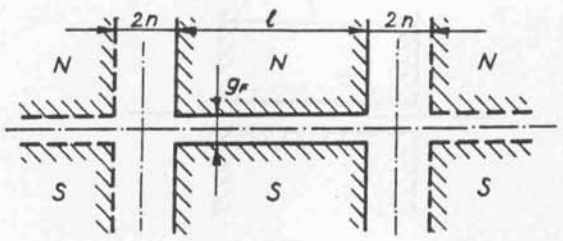

Fig. 10 Approximation of model shown in Fig. 8

simple analytical solution.

If the field line which leads from the point 0_ℓ (Fig 3) on the stator pole end to the rotor end is approximated by a semi-circle with the radius equal to n (see above), then the model in Fig 9 may be approximated by the model shown in Fig 10.

Then the effective core length which takes into account fringe flux for this model is

$$\ell_F = (\ell + 2n)\sigma - 2n = \ell + 2n(1-\sigma) \qquad (10)$$

where σ is Carter's coefficient

$$\sigma = \frac{2}{\pi}\left\{ \text{arc tan}\left(\frac{2n}{g_F}\right) - \frac{g_F}{4n} \ln \left[1 + \left(\frac{2n}{g_F}\right)^2\right]\right\} \qquad (11)$$

For the machine with proportions shown in Fig 3 and ratio ℓ/d_o equal to unity $\ell_F/\ell = 1.17$ which means that the flux-linkage at the ends of core at the minimum inductance position is 14.5% of the total flux-linkage.

3.4 Comparison Between Computed and Measured Results

The value of the minimum inductance on actual machine with typical proportions was computed using the method presented above and by the 2-dimensional boundary integral numerical method developed by Trowbridge and Simkin at the SRC Rutherford Laboratory.

When the fringe flux at the ends of core is excluded, the difference between the estimated value of inductance using the above method and that computed by 2-dimensional numerical field solution is only + 3%. Such excellent agreement indicates that the value of minimum inductance, when the fringe flux at the ends of core is excluded, may be very accurately estimated using the simple analytical method.

The comparison of the estimated value of minimum inductance which includes fringe flux at the ends of core with that obtained by measurement shows a difference of -14%. The reason for this discrepancy is the very rough approximation for fringe flux at the ends of core. (If, for example, the value of n in Fig 10 is doubled then the difference is reduced to -9%.) If this difference is expressed as a percentage of the inductance component due to the fringe flux* it is 50%, ie the estimated value of inductance component due to fringe flux is half the measured value. Using this empirically obtained factor the corrected value of minimum inductance is

$$L_o = L_{2D} + 2L_F = L_{2D} + 2\left(\frac{\ell_F}{\ell} L_{2D} - L_{2D}\right)$$

$$= L_{2D}\left(2\,\frac{\ell_F}{\ell} - 1\right) \qquad (12)$$

where L_{2D} is the estimated value of minimum inductance when the fringe flux is excluded and L_F is the estimated value of inductance component due to fringe flux.

Work is continuing on this problem of estimating the contribution of the fringing field and it is hoped to have available soon results of a 3-dimensional numerical field solution.

4. ESTIMATION OF THE MAXIMUM INDUCTANCE USING B-H CURVE

In the maximum inductance position the mmf drop in the iron is considerable, even in the case when the iron is not saturated, in comparison with mmf drop in the air-gap (the air-gap length is small compared with the rotor diameter). When the iron becomes saturated the mmf drop in the iron increases nonlinearly and may exceed the mmf drop in the air-gap. Therefore the mmf drop in the iron and the nonlinearity of B-H curve of iron must be taken into account for the estimation of the maximum inductance.

To estimate the maximum inductance L_i by a simple analytical method the following assumptions are made:

i) When a phase winding is excited the magnetic circuit is treated as a simple '2-pole' pattern (Fig 11);

* The inductance component due to fringe flux can be obtained as the difference between the measured value of inductance and the one obtained by 2-dimensional numerical field solution

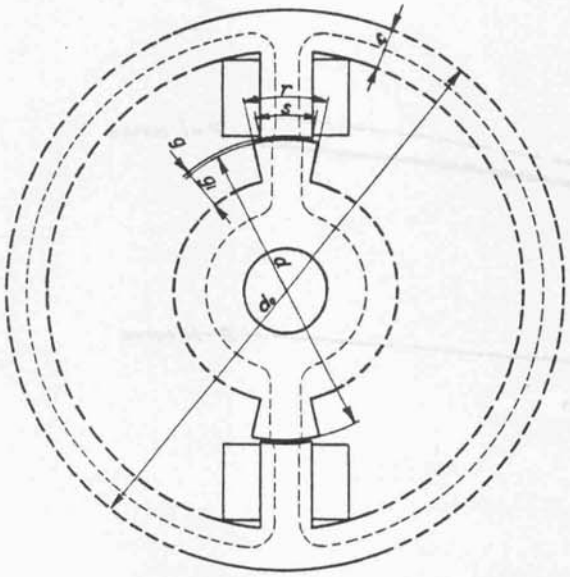

Fig. 11 Simple '2-pole' pattern

ii) There is no flux leakage, ie all flux passes from the stator to the rotor and back;

iii) The flux is linked with all the turns;

iv) The flux is uniformly distributed in the cross-section normal to the field lines.

In the maximum inductance position the field pattern is symmetrical about the axis of the excited phase and therefore only one half of the magnetic circuit, which carries one half of the total flux, need be considered. Further simplification is to split this half of the magnetic circuit into the following parts connected in the series:

two stator poles (subscript 's') with
cross-section: $a_s = \frac{d}{2}(\sin\frac{s}{2})\ell$
length : $\ell_s = 2(\frac{d_o}{2} - c - \frac{d}{2} - g)$

two air-gaps (subscript 'g') with
cross-section*: $a_g = [\frac{1}{2}(\frac{D}{2} + g)s + (1 - \sigma)i]\ell$
where : $i = \frac{1}{2}\frac{D}{2}(r-s)$
$\sigma = \frac{2}{\pi}[\arctan(\frac{i}{g}) - \frac{g}{2i}\ln(1 + (\frac{i}{g})^2)]$
length : $\ell_g = 2g$

two rotor poles (subscript 'r') with
cross-section**: $a_r = a_g$
length : $\ell_r = 2g_i$

rotor body (subscript 'b') with
cross-section : $a_b = (\frac{d}{2} - g_i)\ell$
length : $\ell_b = \frac{1}{2}(\frac{d}{2} - g_i)\pi$

stator yoke (subscript 'y') with
cross-section : $a_y = c\ell$
length : $\ell_y = \frac{1}{2}(d_o - c)\pi$

(The numerical results are related to the machine with the parameters given above.)

The mmf equation is

$$Ni = \frac{B_g}{\mu_o}\ell_g + H_s\ell_s + H_r\ell_r + H_b\ell_b + H_y\ell_y$$

Having given the value of flux-linkage, the values of flux densities B_g, B_s, B_r, B_b and B_y can be calculated ($B = \frac{\psi}{Na}$) and using the B-H curve of the appropriate steel the values for H_s, H_r, H_b and H_y can be found. Using the mmf equation the value of current corresponding to a given value of flux-linkage can be found and hence the maximum inductance if $L_i = \frac{\psi}{i}$. The normalised equivalent maximum permeance is given by

$$P_i = \frac{L_i}{\mu_o \ell N^2}$$

Bearing in mind that the above simple analytical method treats a very simplified field pattern, the error which is within 5% in the highly saturated region of ψ-i curve (in terms of inductance) is very good (Fig 12). In the nonsaturated region the estimated and measured results are very close. Extremely good agreement between the measured ψ-i curve of the maximum inductance position and the one obtained by using 2-dimensional numerical field solution shows that the fringe flux at the ends of core is negligible compared with the flux within machine. It is very interesting to note that the fringe flux at the ends of core in the maximum inductance position is smaller (in absolute value) than the one in the minimum inductance position.

* Due to fringing effects the effective cross-section in the air-gap is bigger than the stator pole cross-section. To make some allowance for this the air-gap cross-section is increased by introducing Carter's coefficient

** It is assumed that the rotor pole cross-section is constant along the rotor pole and equal to effective cross-section in the air-gap (a_g)

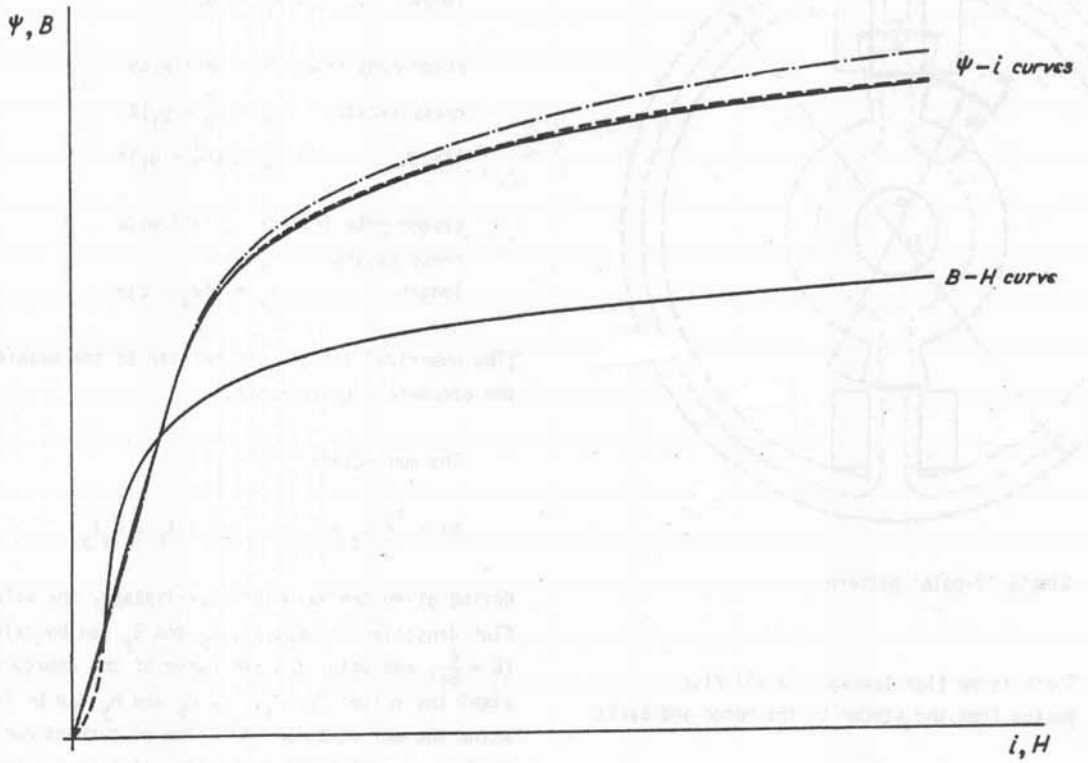

Fig. 12 B-H curve and ψ-i curve in maximum inductance position

——— measured
– – – – computed by numerical field solution
—·— estimated by simple analytical method

5. CONCLUSIONS

A method for the analytical estimation of the minimum and maximum inductances has been given which is valid for realistic saturation in the iron. The method is sufficiently simple to allow it to be programmed on a programmable calculator.

The estimation of the minimum inductance is based on the assumption that the field lines consist of circular arcs and straight line segments. The distribution of the winding is allowed for. The estimated value of minimum inductance, when the fringe flux at the ends of core is excluded, agrees very well (within 3%) with the result obtained by 2-dimensional numerical field solution. An allowance based on a rough approximation for fringe flux at the ends of core has been made. The estimated value of total minimum inductance is 14% lower than measured value. An empirical formula for the corrected value of minimum inductance has been suggested.

In the maximum inductance position the machine is treated as a simple 2-pole pattern and it is assumed that the flux is linked with all turns and there is no flux leakage. The B-H curve of the iron is used in calculating the maximum inductance. The difference between measured and estimated values of the maximum inductance is within 5% in the saturated region of the ψ-i curve and is insignificant in the nonsaturated region.

6. ACKNOWLEDGEMENTS

The authors wish to thank Dr N N Fulton and other colleagues in the Department of Electrical and Electronic Engineering of the University of Leeds for helpful discussions and in the SRC Rutherford Laboratory for their assistance in producing numerical field solutions. J Čorda is indebted to the University for scholarship support.

7. REFERENCES

1. F W Carter; 'The magnetic field of the dynamo-electric machine', Jour IEE, 1926, pp 1115-1138
2. K C Mukherji, S Neville; 'Magnetic permeance of identical double slotting', Proc IEE, Vol 118, No 9, Sept 1971, pp 1257-1268

3. P A Ward and P J Lawrenson; 'Magnetic permeance of doubly-salient air-gaps', Proc IEE, Vol 126, No 6, June 1977, pp 542-543

4. A L Jones; 'Permeance model and reluctance force between toothed structures', Proc of 5nd symposium on incremental motion control system and devices', University of Illinois, May 1976, paper H

5. H D Chai; 'Permeance model and reluctance force between toothed structures', Proc of the 2nd symposium on incremental motion control system and devices, University of Illinois, May 1973, paper K